

United Nations Educational Scientific and Cultural Organization
and
International Atomic Energy Agency

THE ABDUS SALAM INTERNATIONAL CENTRE FOR THEORETICAL PHYSICS

**REALISTIC MODELLING OF THE EFFECTS OF ASYNCHRONOUS MOTION
AT THE BASE OF BRIDGE PIERS**

F. Romanelli¹

Department of Earth Sciences, University of Trieste,
Via Weiss 4, 34127 Trieste, Italy

G.F. Panza and F. Vaccari

Department of Earth Sciences, University of Trieste,
Via Weiss 4, 34127 Trieste, Italy

and

The Abdus Salam International Centre for Theoretical Physics, SAND Group,
Trieste, Italy.

MIRAMARE – TRIESTE

November 2002

¹ Corresponding author: Tel: +39-040-6762116; Fax: +39-040-6762111; E-mail: romanel@dst.univ.trieste.it

ABSTRACT

Frequently long-span bridges provide deep valley crossings, which require special consideration due to the possibility of local amplification of the ground motion as a consequence of topographical irregularities and local soil conditions. This does in fact cause locally enhanced seismic input with the possibility for the bridge piers to respond asynchronously. This introduces special design requirements so that possible out-of-phase ground displacements and the associated large relative displacements of adjacent piers can be accommodated without excessive damage. Assessment of the local variability of the ground motion due to local lateral heterogeneities and to attenuation properties is thus crucial toward the realistic definition of the asynchronous motion at the base of the bridge piers.

We illustrate the work done in the framework of a large international cooperation to assess the importance of non-synchronous seismic excitation of long structures. To accomplish this task we compute complete synthetic accelerograms using as input a set of parameters that describes, to the best of our knowledge, the geological structure and seismotectonic setting of the investigated area.

1. Introduction

It is well accepted that one of the most important factors influencing the space variability of the ground motion is the site response. Due to the insurgence of local surface waves and local resonance, the local amplification, or de-amplification, effects can dominate the groundshaking whenever lateral heterogeneities, such as topographical features or soft-sedimentary basins, are present in the vicinity of a site. If a built structure has dimensions greater than the main wavelengths of the ground motion, different parts of its foundations can vibrate out of phase due to the non-synchronous seismic input. The presence of relevant differential motion makes the structure move in an incoherent way with respect to the surrounding ground. For very extended-in-plan structures (e.g. pipelines, bridges) the differential motion can play an important role even in the absence of nearby strong lateral heterogeneity. In fact the so-called wave-passage effect (i.e. the phase shift of the seismic arrivals at the different parts of the structure) is sufficient to generate incoherent motion on a scale length of the order of one hundred meters.

In the engineering practice, a stochastic model is adopted for the description of the spatial variability of the ground motion, which quantifies the out-of-phase effects in terms of so-called coherency functions. The limit of such an approach is that the incoherence effect, the wave-passage effect and the local effect are described separately by statistical spectral models that are stationary in time and homogeneous in space. The generally low reliability of models based on convolutive methods has been discussed in detail, for example, by [1,2,3].

The understanding of the ground motion spatial variability requires the availability of a dense set of signals corresponding to different representative sources. These signals can be obtained either experimentally, installing local, dense, seismic arrays at different sites, or theoretically, computing synthetic seismograms, by means of computer codes, developed from a detailed knowledge of the seismic source process and of the propagation of seismic waves. The cost of the experimental procedure is self-evident and the collection of a significant data set may require a prohibitive amount of time. The limits arising from the use of a theoretical procedure, which is economically very valid and can be performed timely, can be largely reduced using the available records as a benchmark of the synthetic signals. In such a way, realistic seismograms, suitable as seismic input in any engineering analysis, e.g. for the design of earthquake-resistant structures or for the estimation of differential motion, can be computed at a very low cost/benefit ratio. We present an example of the theoretical procedure applied to the seismic hazard assessment of the Warth bridge, near Vienna (Austria), where no seismic records are available. The relevant information about seismic

input is an estimate of the macroseismic intensity, in the range VI-VIII (MSK), the value of the magnitude, 5.5, of the nearest largest recorded event, and the most probable focal depth of strong earthquakes, in the range 6-11 km (e.g. [4]).

2. Definition of source and structural models

To define the possible seismic sources that drive the seismic hazard of the Warth region, we used the database of focal mechanisms developed at the Department of Earth Sciences at the University of Trieste (DST) for the EC project QSEZ-CIPAR (e.g. [5]). Taking into account the magnitudes and the distances from the Warth region, we selected the five sources, whose focal mechanism parameters are listed in Table 1, shown in Figure 1.

As reference bedrock model, a regional structural model for the Vienna basin has been compiled on the base of the I-dataset [6]. The model we consider to be representative of the Warth region is shown in Figure 2.

Starting from the available Warth bridge section plan, a digitized model of the geological cross-section underlying the bridge has been constructed (see Figure 3). On the basis of the geological and geotechnical information available, the elastic and the anelastic parameters have been assigned to the various geotechnical units contained in the section.

3. Definition of the seismic input: calculation of synthetic signals

3.1. Bedrock model analysis

As a first step, synthetic seismograms have been generated by the modal summation technique [7,8,9,1] for the bedrock model. The distances of the selected sources from the Warth bridge site (assumed geographical coordinates: Latitude=47.660°N and Longitude=16.170°E) are respectively 41.2 km, 20.3 km, 26.8 km, 8.6 km and 13.7 km. As a conservative choice, magnitude (5.5) and hypocentral depth (5 km) have been kept constant for all the sources. Here and in the following computations, the source finiteness has been taken into account by properly weighting the source spectrum using the scaling laws of Gusev [10,11]. The computations of synthetic seismograms (displacements, velocities and accelerations for the radial, transverse and vertical components) at the base of each pier have been carried out, with cut-off frequency at 1 Hz and 10 Hz. The differential motions of each pier with respect to the first one and with respect to the preceding pier have been computed. At 1 Hz cut-off frequency, no differential motion could be detected, while at 10 Hz the amplitude of the differential motion becomes comparable with the input motion amplitude.

3.2. Local model analysis

To deal with both realistic source and structural models, including topographical features, a hybrid method has been developed (e.g. [12,13]) that combines modal summation and the finite difference technique, and optimizes the use of the advantages of both methods. With our approach, source, path and site effects are all taken into account, and a detailed study of the wavefield that propagates even at large distances from the epicenter is therefore possible. In the hybrid scheme the local heterogeneous model has been coupled with the average regional model used in the bedrock model analysis. The minimum S-wave velocity in the model is 220 m/s, and the mesh used for the finite differences is defined with a grid spacing of 3 m. This allows us to easily carry out the computations at frequencies as high as about 8 Hz, upper frequency limit that is fully satisfactory for our purposes. The synthetic time signals have been calculated for the three components of motion, adopting the seismic source model SEE72 of Table 1. The focal mechanism parameters are shown in the legend of Figures 4, 5 and 6, that show the acceleration time series for the radial, transverse and vertical component of motion, respectively. The lateral heterogeneity can produce strong spatial variations in the ground motion even at small length scales (the distance between two adjacent signals is approximately ten meters) and also for the vertical component of motion (see Figure 6).

In order to have a conservative estimation of the differential motion, the working magnitude has then been chosen equal to 5.5 (seismic moment equal to $1.8 \cdot 10^{17}$ Nm) that corresponds to the nearest largest recorded event. The differential motion of each pier, with respect to the first one and with respect to the preceding pier, has been computed. The results show that the differential motion amplitude is comparable with the input motion amplitude when displacement, velocity and acceleration are considered. As an example, at the sites corresponding to the piers location, Figures 7, 8 and 9 show the synthetic accelerations (bottom row) and the differential acceleration, with respect to the preceding pier (middle row) and with respect to the first pier (top row). The same procedure has been applied to other variants of the seismic source and cross-section configuration, in order to produce different ground-shaking scenarios. The parameters of the seismic source double-couple models, that have been considered, are described in Table 2 and represented in Figure 10. The synthetic time signals (displacements, velocities and accelerations) have been calculated for the three components of motion, adopting the source models S2 and S3 of Table 2. In order to have a conservative estimation of the differential motion along the bridge, the source is located in the same plane that contains the cross-section (see Figure 10).

As an example, at the sites corresponding to the piers location, Figures 11 and 12 show the synthetic accelerations (bottom row) and the differential acceleration, with respect to the preceding pier (middle row) as well as the one with respect to the first pier (top row), for the radial component of motion, for sources S2 and S3, respectively.

The considerations that have been made about the results obtained using the source model S1 apply here as well: the differential motion amplitude is comparable with the input motion amplitude when displacement, velocity and acceleration are considered. Similar results are obtained with other variants of source and structural models.

4. Conclusions

The assessment of the local variability of the ground motion due to local lateral variations of the elastic and attenuation properties is crucial for the realistic definition of the asynchronous motion at the base of bridge piers. The definition of the seismic input at the Warth bridge site, i.e. the determination of the seismic ground motion due to an earthquake with a given magnitude and epicentral distance from the site, has been done following a theoretical approach. Such an approach is based on modeling techniques, developed from the knowledge of the seismic source process and of the propagation of seismic waves, that can realistically simulate the ground motion associated with the given earthquake scenario.

The results show that lateral heterogeneity can produce strong spatial variations in the ground motion even at small incremental distances. Such variations can hardly be accounted for by the stochastic models commonly used in engineering practice. In absolute terms, the differential motion amplitude is comparable with the input motion amplitude when displacement, velocity and acceleration domains are considered. Thus, on the base of the existing empirical regression relations between Intensity and peak values of ground motion [14,15] a general result of our modeling is that the effect of the differential motion can cause an increment greater than one unit in the seismic intensity experienced by the bridge, with respect to the average intensity affecting the area where the bridge is built.

Acknowledgements

The results are part of the studies that are being carried on for the E. C. Environmental Programme RTD Project ENV4-CT98-0717 "Advanced Methods for Assessing the Seismic Vulnerability of Existing Motorway Bridges (VAB Project)". The international team was made up of seven partners: Arsenal research, Vienna, Austria; ISMES S.P.A., Bergamo, Italy; ICTP, Trieste, Italy; UPORTO, Porto, Portugal; CIMNE, Barcelona, Spain; SETRA, Bagneaux, France; JRC-ISPRA, EU.

We used GMT software [16] in the preparation of Figures 1-2.

References

1. Romanelli, F. and Vaccari, F. (1999). "Site response estimation and ground motion spectral scenario in the Catania Area", *J. of Seism.*, **3**, p. 311-326.
2. Field, E.H., the SCEC Phase III Working Group (2000). "Accounting for site effects in probabilistic seismic hazard analyses of Southern California: overview of the SCEC Phase III report", *Bull. Seism. Soc. Am.*, **90**, 6B, p. S1-S31.
3. Panza, G.F., Romanelli, F. and Vaccari, F. (2001). "Seismic wave propagation in laterally heterogeneous anelastic media: theory and applications to the seismic zonation", *Advances in Geophysics*, Academic press, **43**, 1-95.
4. Lenhardt, W. A. (1998). "Focal mechanisms of recent earthquakes in Austria", ESC Assembly Papers book, 23-28 August Tel Aviv, Israel, 36-40.
5. Suhadolc, P. and Panza, G. F. (1996). "Focal mechanisms and seismogenetic zones", EEC Technical Report, Project CIPA-CT94-0238.
6. Du, Z. J., A. Michellini and Panza, G.F. (1998). "EurID: a regionalized 3-D seismological model of Europe", *P.E.P.I.*, **105**, 31-62.
7. Panza, G.F. (1985). "Synthetic Seismograms: the Rayleigh Waves Modal Summation", *J. Geophys.*, **58**, 125-145.
8. Panza, G.F., Suhadolc, P. (1987). "Complete strong motion synthetics", in *Seismic strong motion synthetics* (B. A. Bolt editor), Academic Press, Orlando, 153-204.
9. Florsch, N., Fäh, D., Suhadolc, P., Panza, G.F. (1991). "Complete Synthetic Seismograms for High-Frequency Multimode SH-Waves", *PAGEOPH*, **136**, 529-560.
10. Gusev, A. A. (1983). "Descriptive statistical model of earthquake source radiation and its application to an estimation of short period strong motion", *Geophys. J. R. Astron. Soc.* **74**, 787-800.
11. Aki, K. (1987). "Strong motion seismology", in M. Erdik and M. Toksöz (eds) *Strong ground motion seismology*, NATO ASI Series, Series C: Mathematical and Physical Sciences, D. Reidel Publishing Company, Dordrecht, Vol. 204, pp. 3-39.
12. Fäh, D., Iodice, C., Suhadolc, P. and Panza, G.F (1993). "A new method for the realistic estimation of seismic ground motion in megacities: the case of Rome", *Earthquake Spectra*, **9**, 643-668.
13. Fäh, D., Suhadolc, P., Mueller, St. and Panza, G.F. (1994). "A hybrid method for the estimation of ground motion in sedimentary basins: quantitative modeling for Mexico City", *Bull. Seism. Soc. Am.*, **84**, 383-399.
14. Aptikaev F.F. (2001). "Strong Ground Motion Due to Earthquakes (in Russian)", Doctoral Thesis. United Institute of Physics of the Earth, Moscow.
15. Panza G.F., Vaccari F., Cazzaro R. (1999). "Deterministic seismic hazard assessment", In: *Vrancea earthquakes: tectonics, hazard and risk mitigation* (F. Wenzel F. et al. Editors), Kluwer Academic Publishers. Netherlands. 269-286.
16. Wessel, P., and Smith, W.H.F. (1991). "Free software helps map and display data", *EOS Trans. AGU*, **72**, 441.

Table 1. Focal mechanisms for the five selected sources.

Source	Lon E (°)	Lat N (°)	Focal Depth (km)	Strike (°)	Dip (°)	Rake (°)	Magnitude Ms (Mb)
SEM63	16.200	48.030	?	180	20	90	?
SEM64_1	15.920	47.730	3	90	81	311	(4.7)
SEM64_2	15.950	47.850	1	100	70	31	(5.4)
SEE72	16.120	47.730	18	190	70	324	5.5 (4.9)
NEU72	16.020	47.730	19	127	80	190	4.4

Table 2. Parameters of the seismic source double-couple models.

Source identification	Focal depth (km)	Distance (km)	Strike (°)	Dip (°)	Rake (°)	Magnitude Ms
S1	5	~9	190	70	324	5.5
S2	5	~9	10	70	324	5.5
S3	5	50	190	70	324	6.0

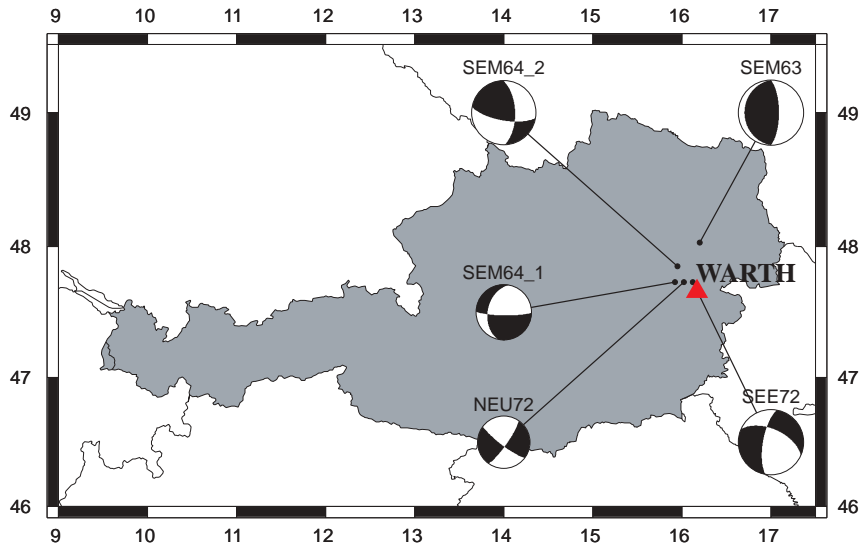


Figure 1. Focal mechanisms of the 5 events reported in Table 1 and Warth site (triangle).

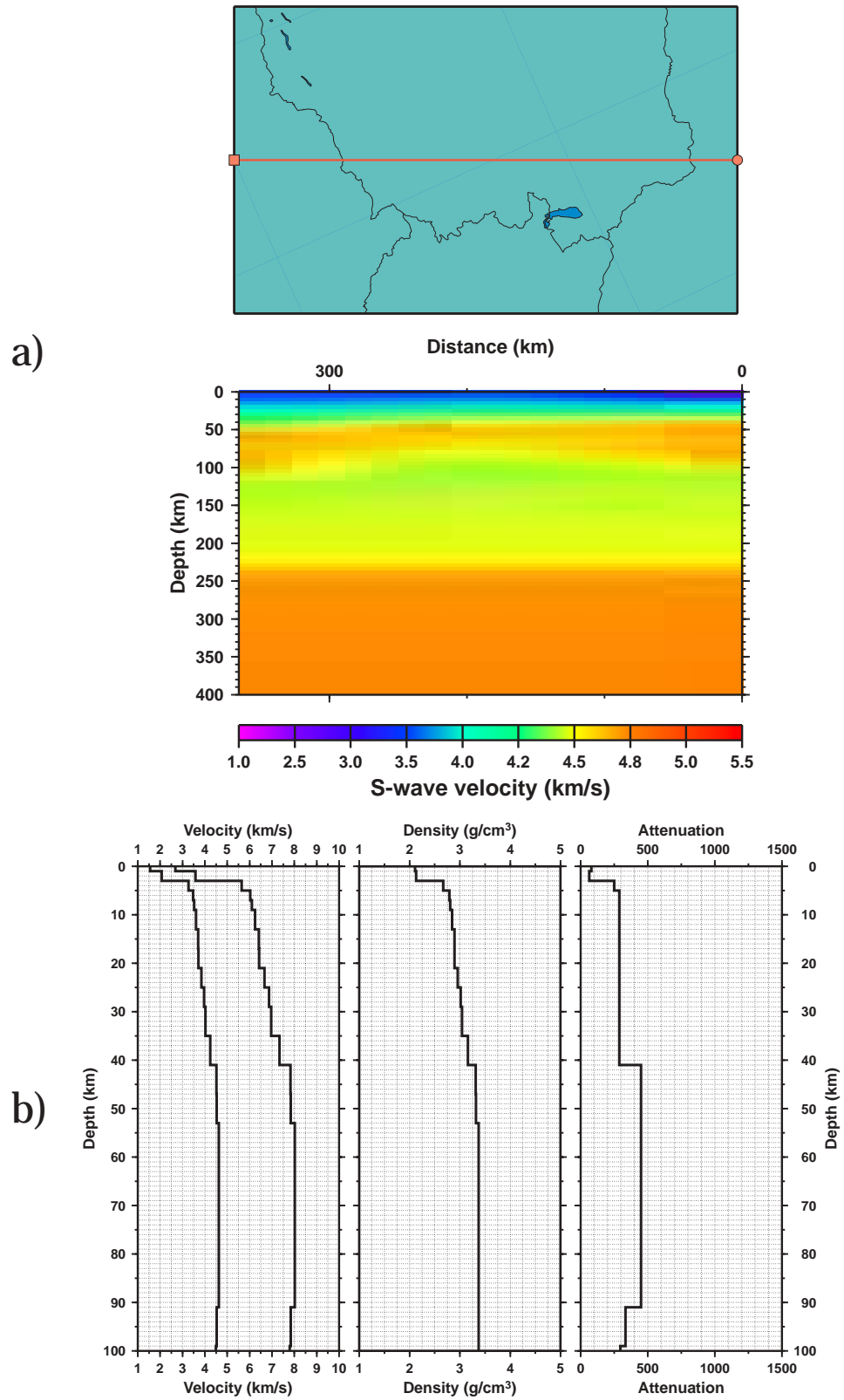


Figure 2. a) Cross-section from EUR-I dataset; b) average reference bedrock model. Attenuation is expressed by Q factor.

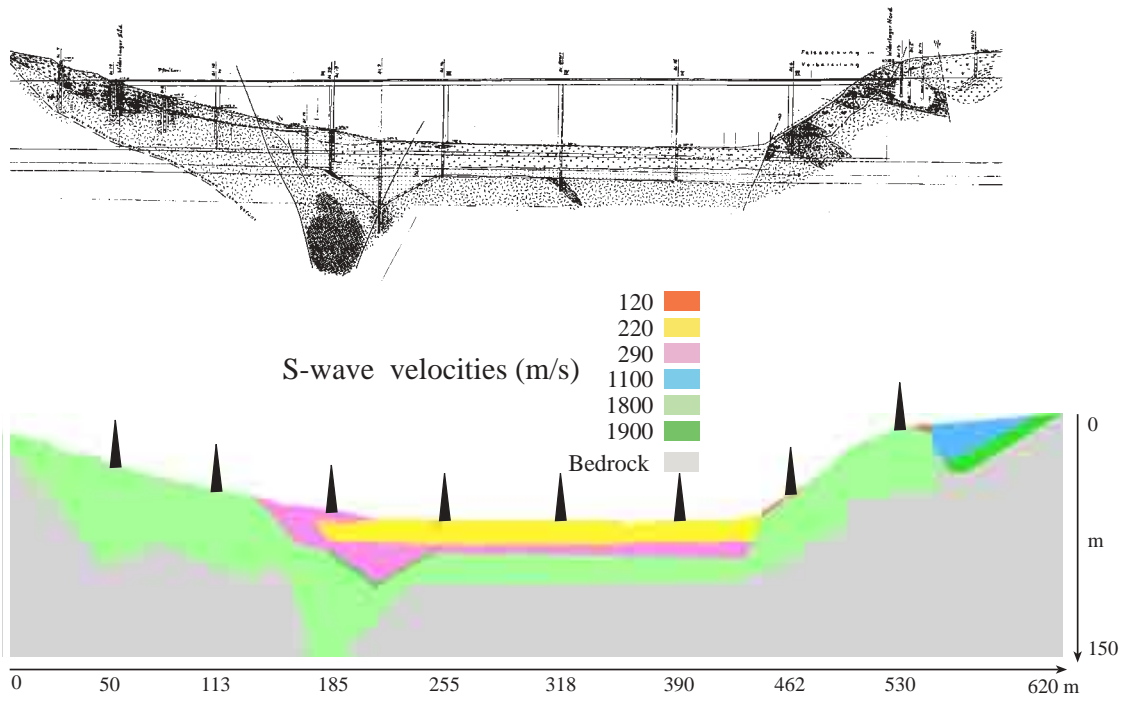


Figure 3. Laterally heterogeneous local model along Warth bridge. Black triangles show the sites of the abutments and of the piers.

Radial acceleration

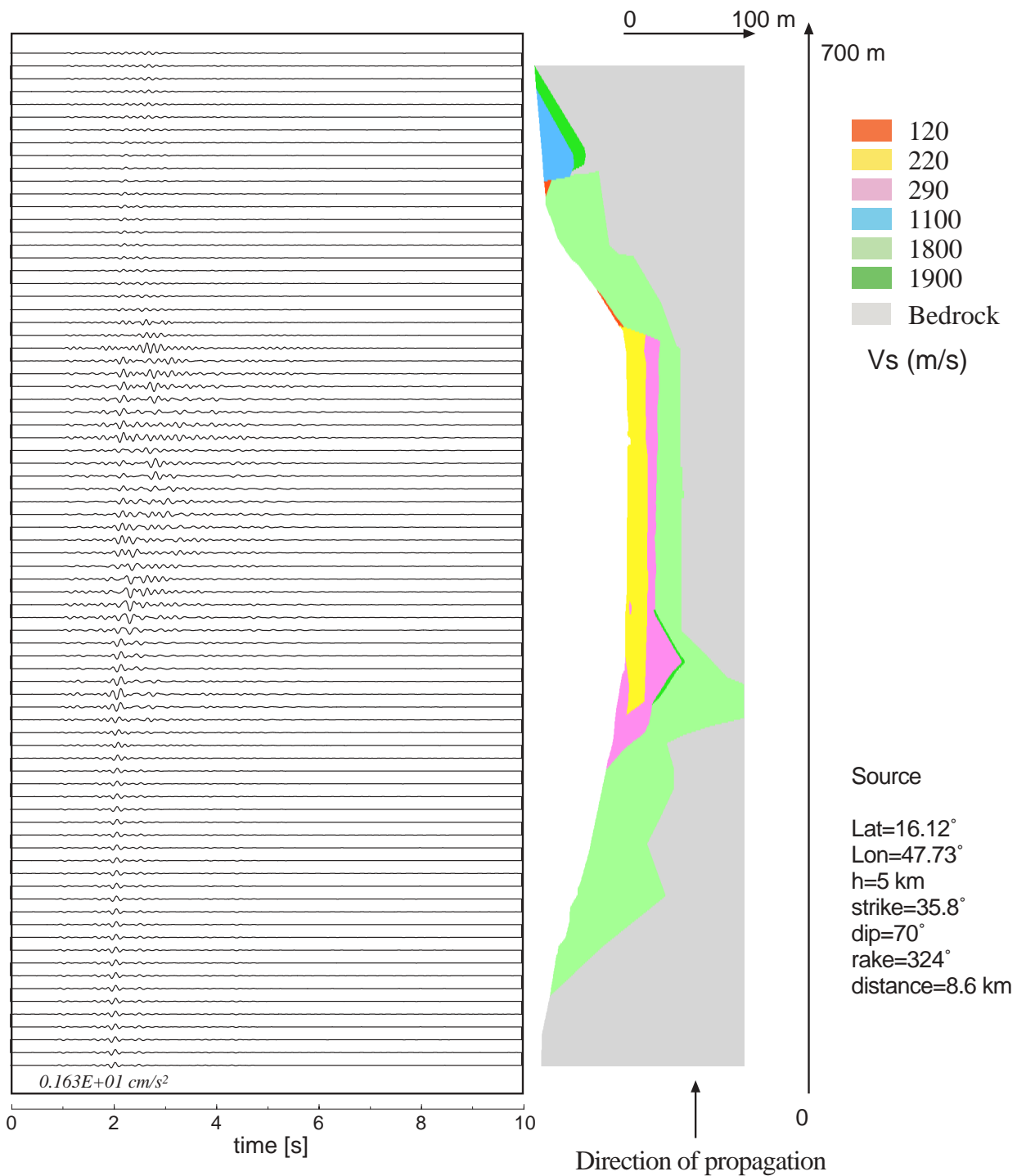


Figure 4. Acceleration time series corresponding to the radial component of motion and to a seismic source with scalar moment of 10^{13} Nm.

Transverse acceleration

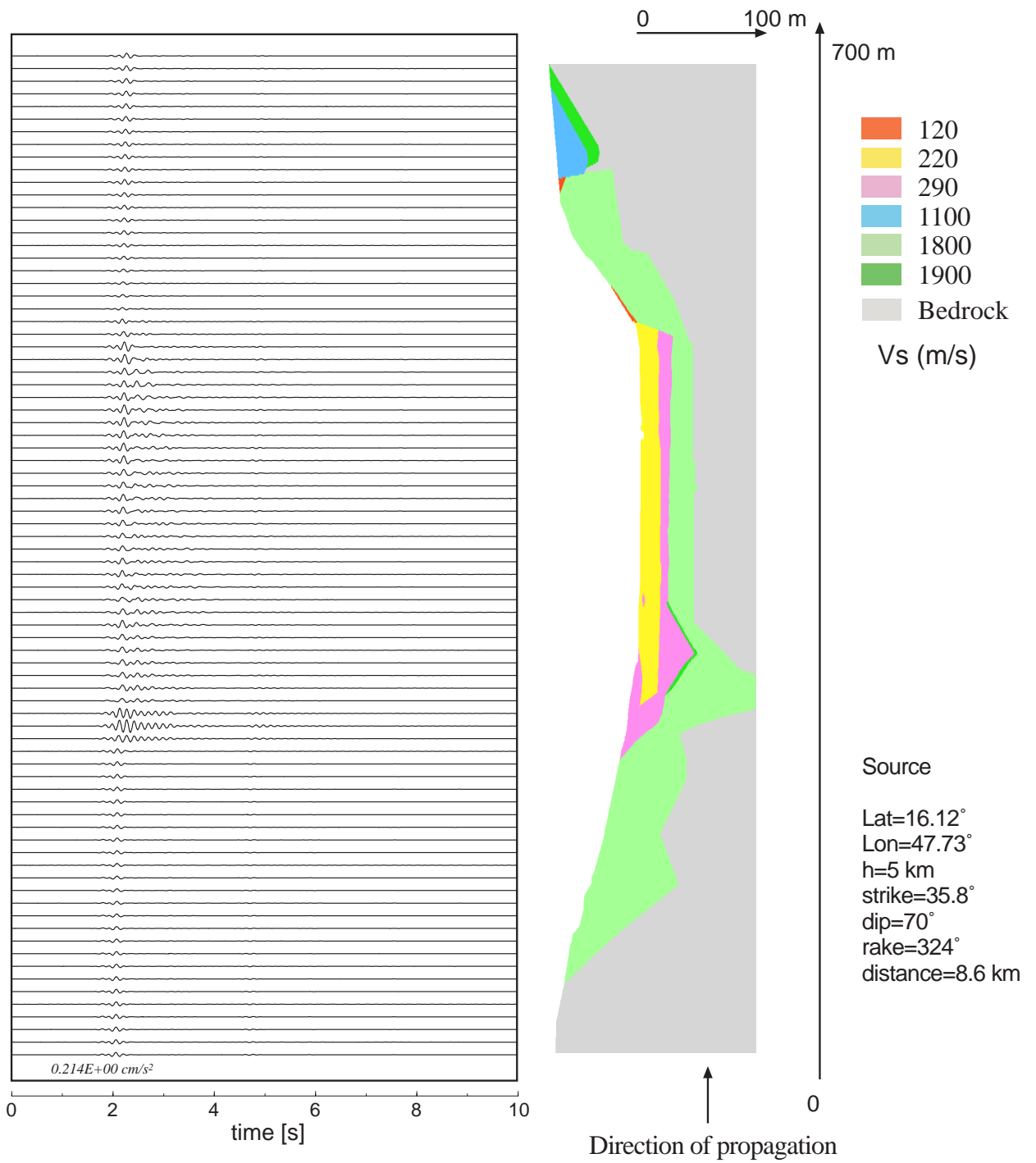


Figure 5. Acceleration time series corresponding to the transverse component of motion and to a seismic source with scalar moment of 10^{13} Nm.

Vertical acceleration

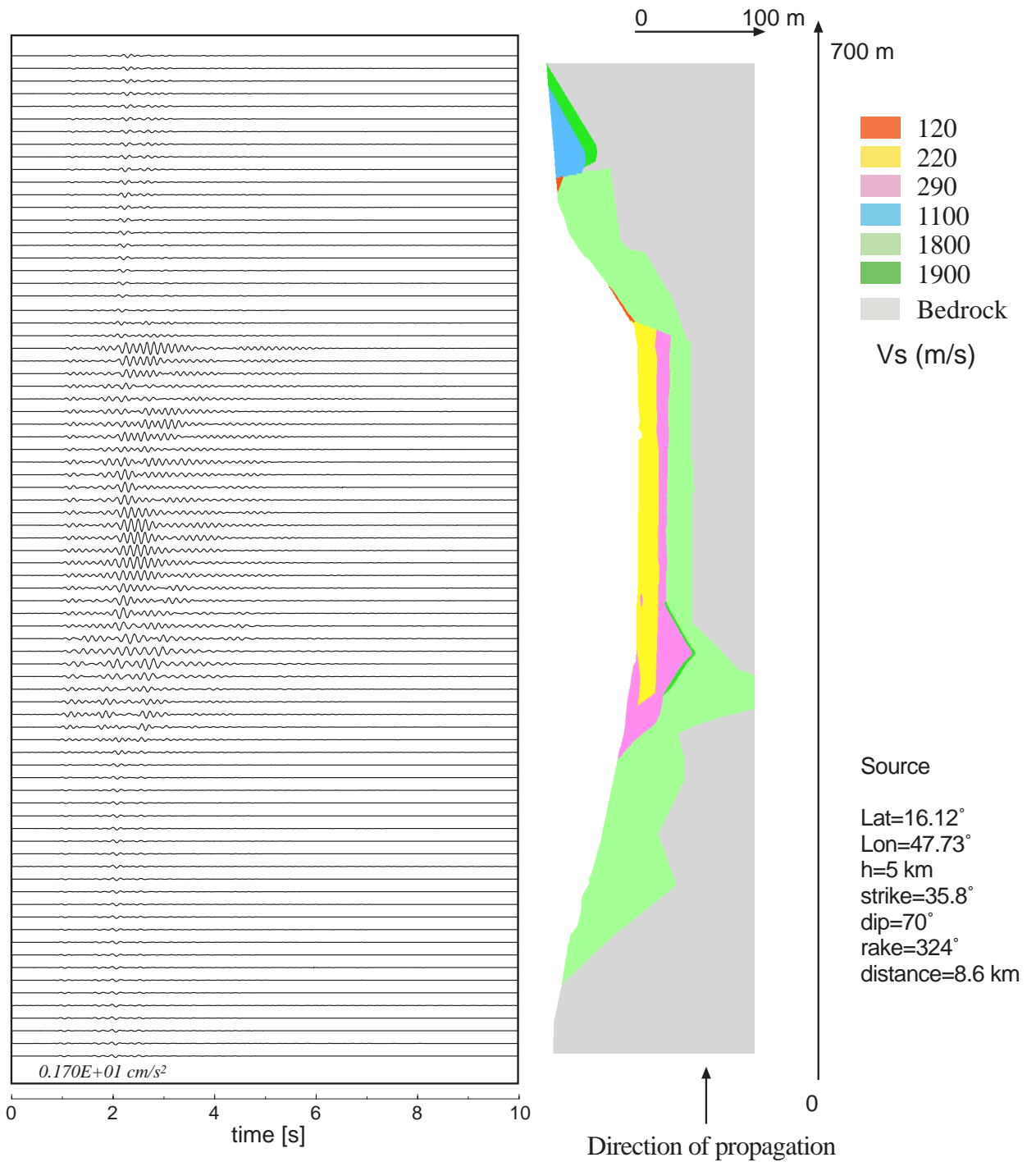


Figure 6. Acceleration time series corresponding to the vertical component of motion and to a seismic source with scalar moment of 10^{13} Nm.

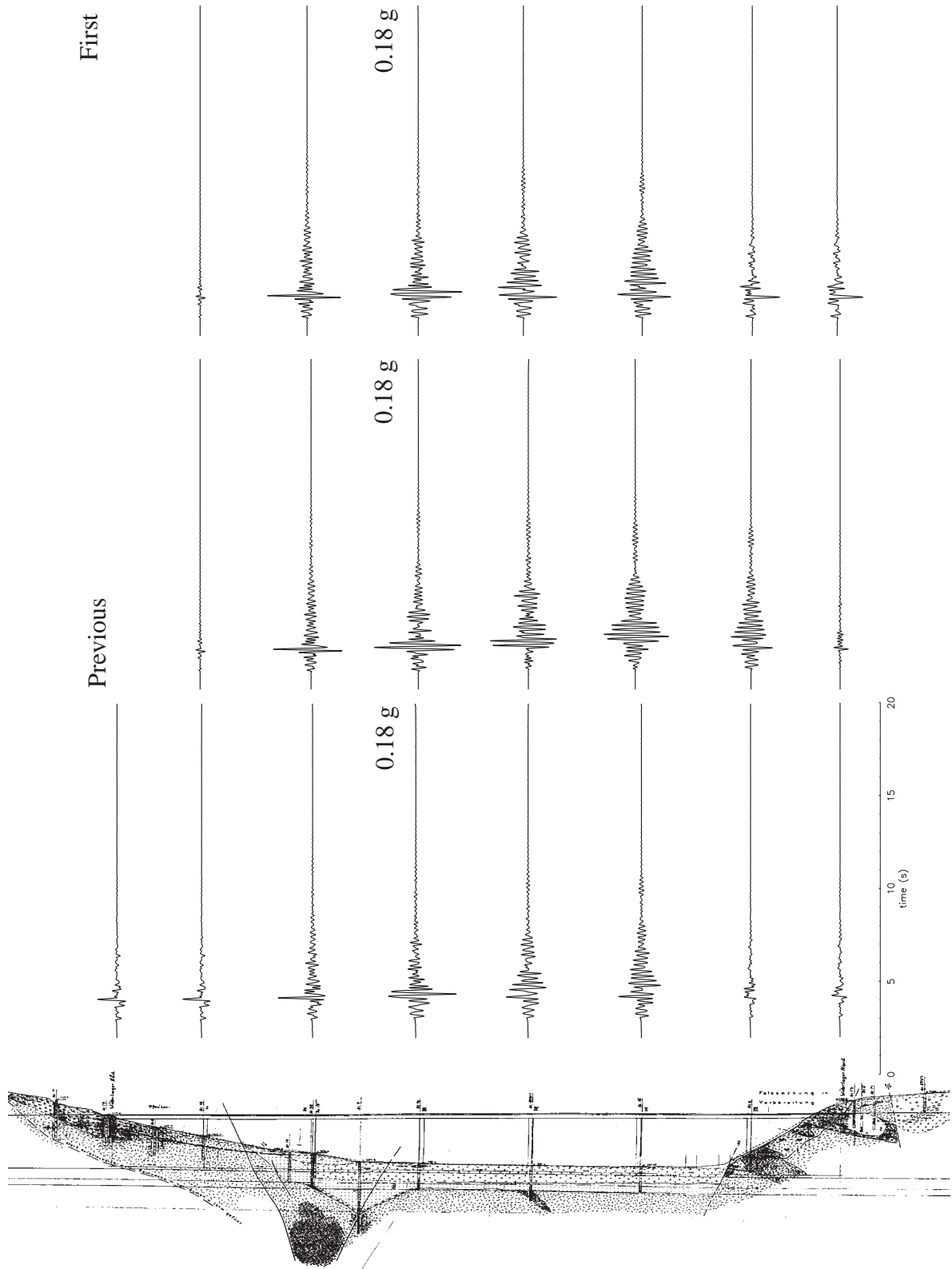


Figure 7. Synthetic accelerations (bottom row) and the differential acceleration, with respect to the preceding pier (middle row) as well as the one with respect to the first pier (top row), at the sites corresponding to the piers location, for the radial component of motion.

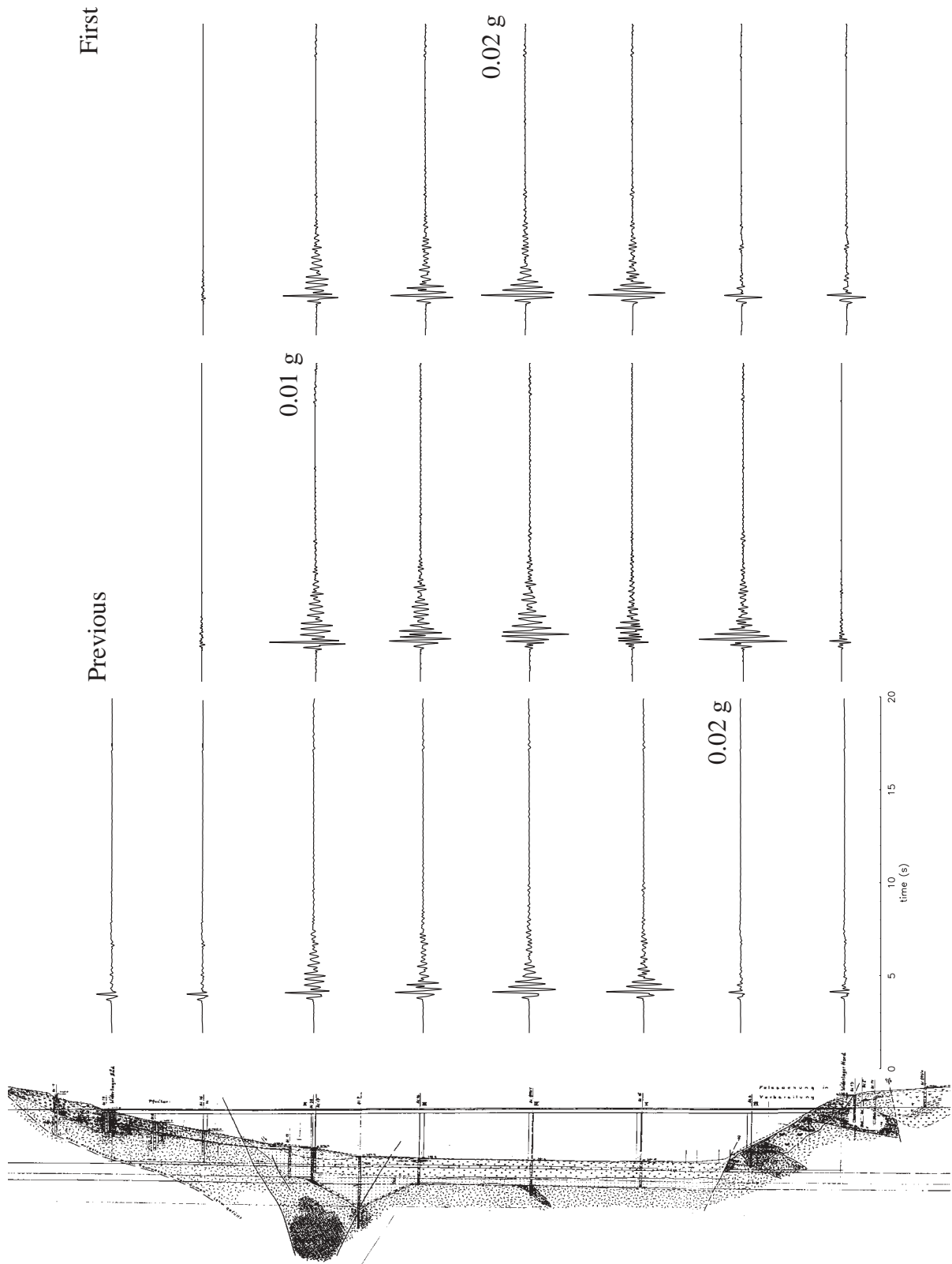


Figure 8. Same as for Figure 7 but for the transverse component of motion.

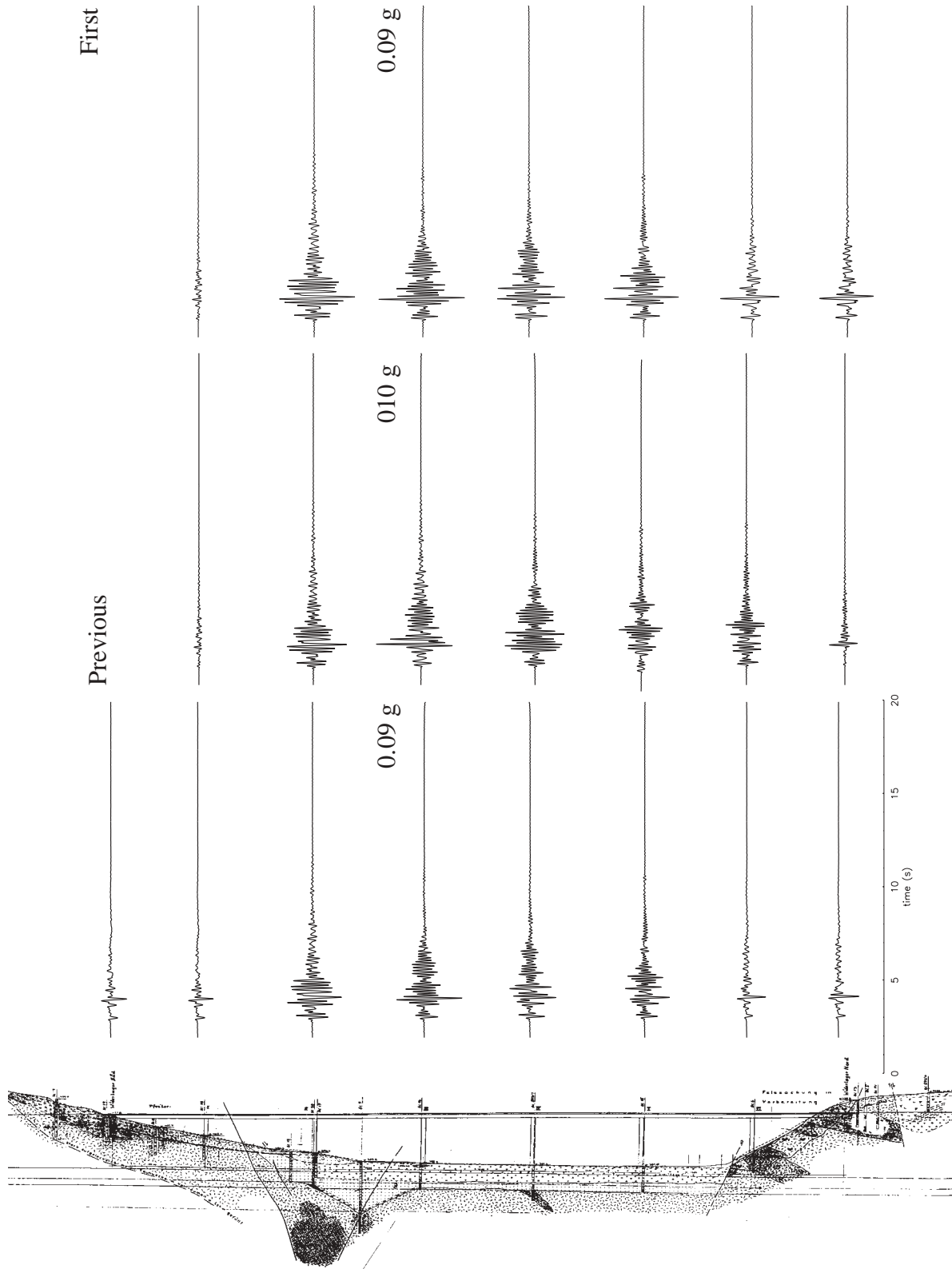
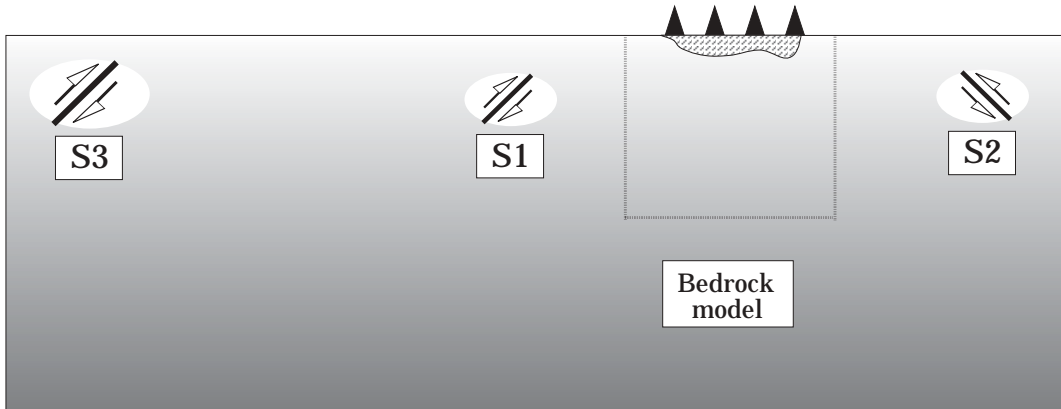


Figure 9. Same as for Figure 7 but for the vertical component of motion.



S3
 Mw = 6.0
 Distance = 50 km

S1
 Strike = 190°
 Dip = 70°
 Rake = 324°
 Depth = 5 km
 Mw = 5.5
 Distance = 8.7 km

S2
 Mw = 5.5
 Strike = 10°

Figure 10. Different configurations adopted in the analysis (see Table 2).

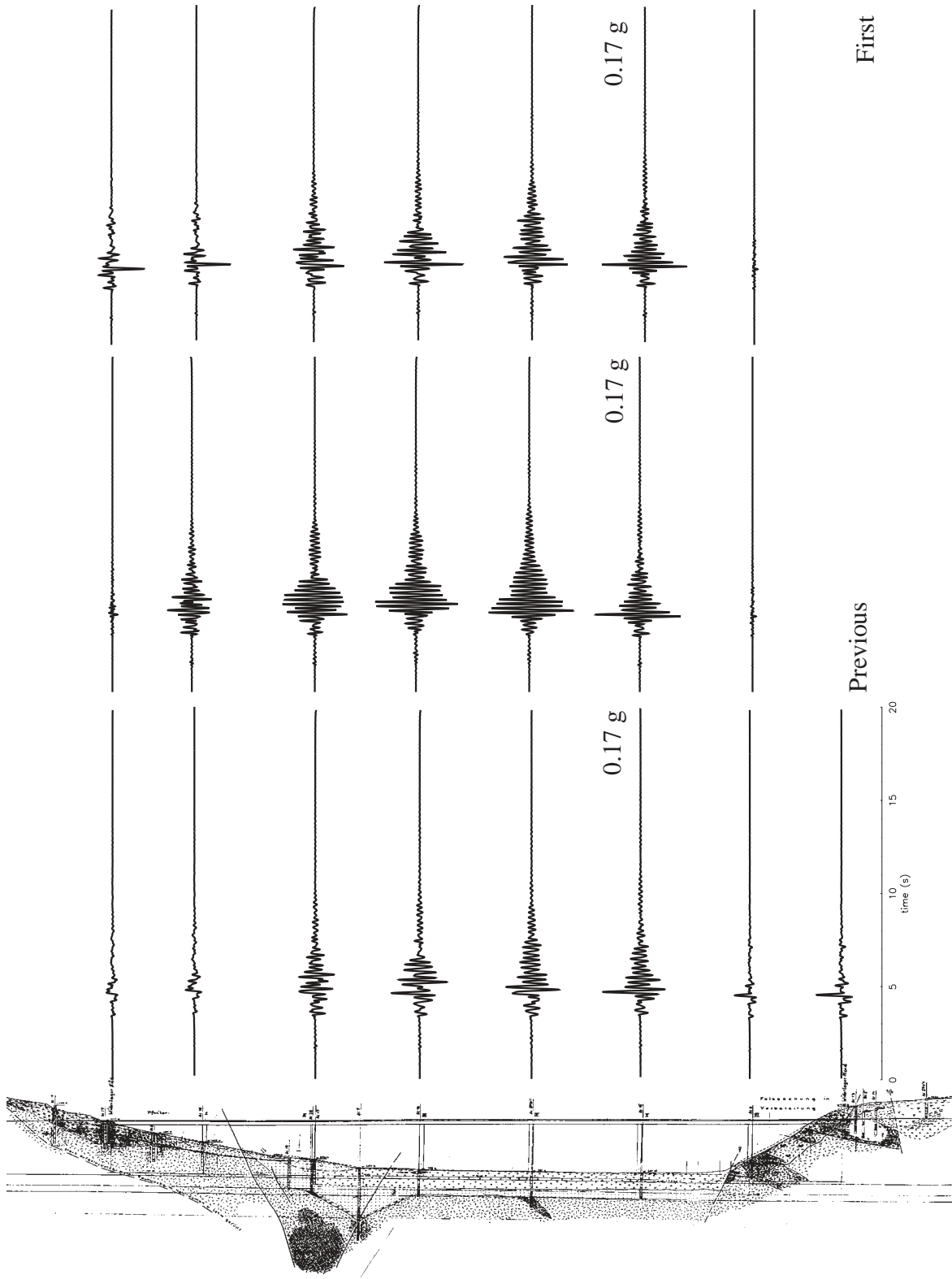


Figure 11. Synthetic accelerations (bottom row) and the differential acceleration, with respect to the preceding pier (middle row) as well as the one with respect to the first pier (top row), at the sites corresponding to the piers location, for the radial component of motion and source S2.

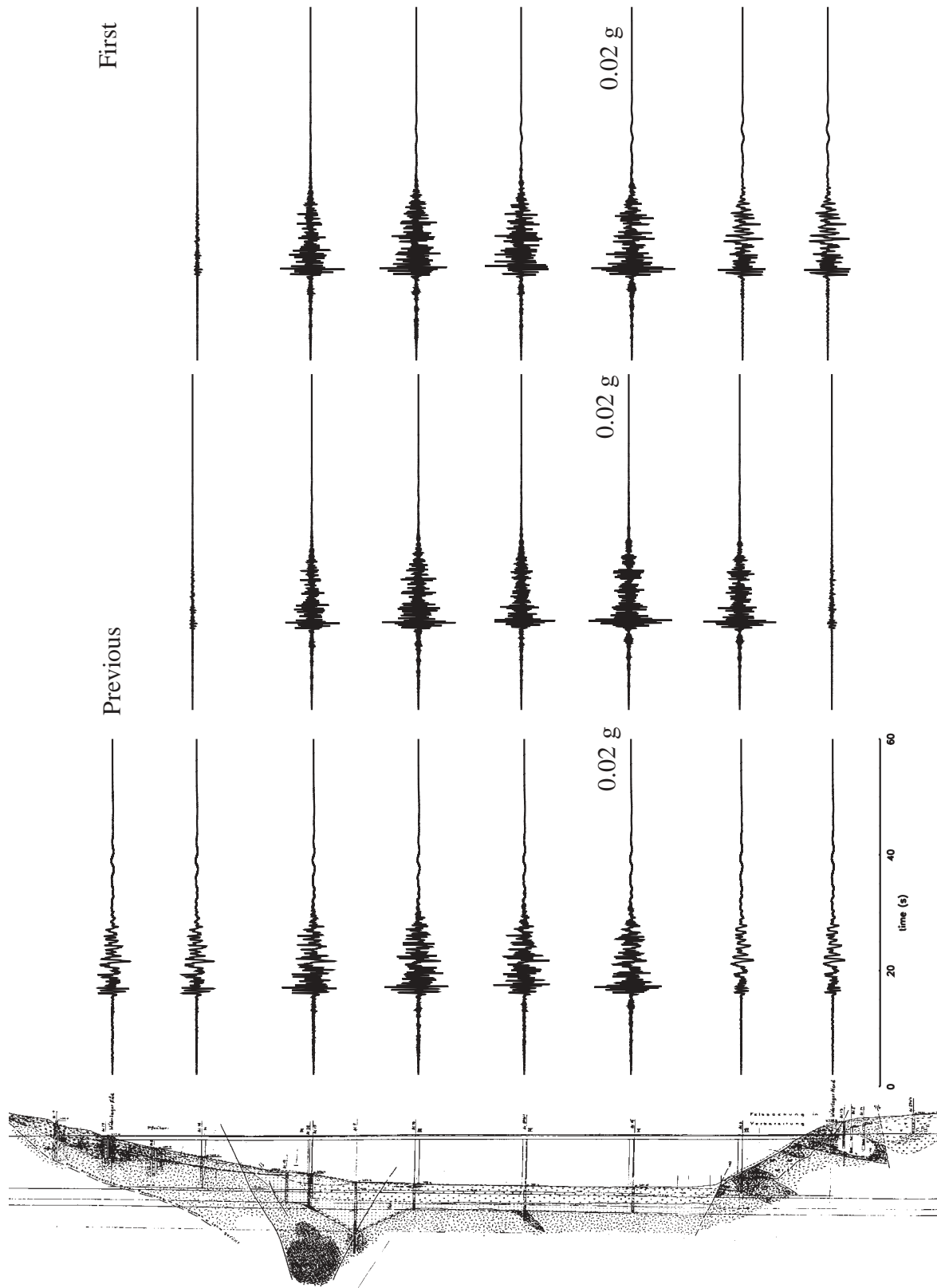


Figure 12. Same as Figure 11 but for source S3.